

Structural characterization of chia seed polysaccharides and evaluation of its immunomodulatory and antioxidant activities

Zhijun Xiao^{a,1}, Changyang Yan^{a,1}, Chunxue Jia^a, Ying Li^b, Yuanlin Li^a, Jie Li^a, Xinxin Yang^a, Xueyan Zhan^{a,*}, Changhua Ma^{a,*}

^a School of Chinese Materia Medica, Beijing University of Chinese Medicine, Beijing 100029, China

^b Department of Pharmacy, The First Affiliated Hospital, and College of Clinical Medicine of Henan University of Science and Technology, Luoyang 471003, China

ARTICLE INFO

Keywords:

Chia seeds polysaccharide
Homogeneous polysaccharide
Structure characterization
Antioxidants
Immunomodulatory activity
Functional food

ABSTRACT

This study aims to extract an active heteropolysaccharide Chia seed polysaccharide (CSP-A) and further purified by DEAE Sepharose Fast Flow and Sepharose CL-6B chromatographic column, characterize its structure, and evaluate its antioxidant and immunomodulatory activities. Structural analysis revealed that CSP-A was composed of D-mannose, D-glucuronic acid and D-xylose in a molar ratio of 1:3:4 with molecular weight of 1.688×10^5 Da, owning 4 sugar residues of β -D-Manp-(1 \rightarrow , \rightarrow 4)- α -D-GlcpA-(1 \rightarrow , \rightarrow 2,4)- β -D-Xylp-(1 \rightarrow , and \rightarrow 4)- β -D-Manp-(1 \rightarrow). Congo red assay and microscopic characteristics showed that CSP-A in its solution may possess a helical conformation. In vitro experiments showed that CSP-A had moderate DPPH- and OH- scavenging activities. CSP-A also enhanced the phagocytosis ability of RAW 264.7 cells and prompted the release of NO, TNF- α , IL-6 and IL-1 β from RAW 264.7 cells, which indicated CSP-A had immune regulation effect. This experiment provides scientific basis for further utilization and development of chia seeds, a kind of functional food.

Introduction

Chia seeds, the seed of *Salvia hispanica* L. belong to Labiateae, which is originally planted in the area of ancient Central America and has been used as a natural nutritional supplement by the natives since 1500 BCE (Ayerza & Coates, 2004), is native to southern Mexico and Guatemala in North America, and now widely planted in Ecuador, Australia and Argentina, with a long history of food and cultivation (Steffolani, Martínez, León, & Gómez, 2015). Recent studies have shown that the chemical composition of Chia seeds mainly includes protein, fatty acids, carbohydrates, dietary fiber, mineral elements, ash and a variety of antioxidant components (Ixtilana, Nolasco, & Tomás, 2008). Chia seeds has significant preventive and therapeutic effects on cardiovascular diseases, obesity and diabetes, such as lipid-lowering, antioxidant, cardiovascular improvement and weight loss (Alfredo, Gabriel, Luis, & David, 2009). As a “super food”, Chia seeds has been widely used in the pharmaceutical, food and cosmetic industries now. Some studies have found that chia seed extract has obvious antioxidant bioactivity and can

be used as a potential natural antioxidant to improve the antioxidant status and reduce lipid peroxidation in obese rats (Rafaela, Lenquiste, Moraes, & Maróstica, 2015). In addition, chia seeds can reduce the risk of cardiovascular diseases and improve the disorder of lipid metabolism. The rich dietary fiber in chia seeds plays a role in lowering blood sugar and blood pressure (Rossi et al., 2013, Toscano et al., 2014, Vladimir et al., 2007). Chia seeds polysaccharides (CSP) are a kind of important bioactive substances in Chia seeds, having many kinds of significant physiological functions and broad prospects of development and application.

In recent years, natural plant polysaccharides have attracted much attention from researchers in the food and biomedical fields (Xie et al., 2013). Polysaccharide is a kind of natural biological macromolecule. Great progress has been made in its extraction, removal, separation, purification and structural characterization, which has laid a foundation for exploring the biological activity of polysaccharide. The main biological activities of polysaccharides include hypoglycemic, immune-enhancing, antibacterial, antioxidant, anti-tumor and anti-radiation

* Corresponding authors at: School of Chinese Materia Medica, Beijing University of Chinese Medicine, No. 11, North Third Ring East Road, Chaoyang District, 100029 Beijing, China.

E-mail addresses: xiao15109141415@sina.com (Z. Xiao), Yan18203074164@163.com (C. Yan), a15242876702@163.com (C. Jia), lyl73885136@163.com (Y. Li), lijie123xyd@163.com (J. Li), 1219463857@qq.com (X. Yang), snowzhan@bucm.edu.cn (X. Zhan), machanghua60@sina.com (C. Ma).

¹ Co-first author, these two authors contributed equally to this work and should be co-first authors.

(Gong et al., 2018). Many natural polysaccharides have free radical scavenging activity and play an antioxidant role. Chuanminshen violaceum polysaccharides has the ability to clear DPPH, O²⁻ and OH⁻, increase the activity of antioxidant enzymes in mice, improve the antioxidant activity of aging mice, and exert the antioxidant effect of polysaccharide (Fan et al., 2017). Astragalus polysaccharide can induce mouse macrophage RAW264.7 to release cytokine and NO through the activation of NF-κB and MAPK mediated by TLR4, and up-regulate the expression of IL-6, TNF-α and iNOS genes, thus playing the immunomodulatory role of polysaccharide (Wei et al., 2016). In addition, Angelica polysaccharides, bupleurum polysaccharides, yam polysaccharides and Prunella polysaccharides can exert immunomodulatory activities through different pathways (Cheng, 2008; Luo et al., 2016). In addition, polysaccharides based nanoparticles, hydrogels or adjuvants have unique advantages in the field of functional food and medicine (Kou et al., 2023). The nano-composite hydrogels prepared with polysaccharide as the matrix have stronger properties and promote wound healing than traditional wound dressings (Zhang, Liu, & Li, 2023). The drug delivery materials prepared with natural polysaccharides as raw materials for the treatment of common colon diseases can realize the accurate release of drugs in the colon, reduce the drug dose and systemic adverse reactions (Wang et al., 2023). Moreover, with the change of people's eating habits, the application of natural polysaccharides in food raw materials can also regulate intestinal microbes, promote in vitro digestion, and improve diet-induced obesity (Tan, Wang, & Chen, 2023). Based on the many advantages of polysaccharides, it is important to further explore the structure and biological activity of polysaccharides in functional foods.

CSP also known as chia seeds gum (CSG), is a water soluble heteropolysaccharide (molecular weight 800 ~ 2000 kDa) derived from the seed coat of chia seeds. As a healthy natural gel, CSP are widely used as food additives, cosmetics and nutrition supplements. The current research on CSP mainly focuses on its emulsification, water holding capacity, viscosity and part of the polysaccharides structure, and there are few reports on the systematic isolation and purification, structure and activities characterization of CSP (Capitani et al., 2015; Fernandes et al., 2017). In this work, a class of CSP was extracted, isolated, purified and characterized according to the current systematic polysaccharide research methods. At the same time, the antioxidant activity and immune activity of the CSP were evaluated in vitro, which could provide experimental basis for further research of the polysaccharide and provide certain guidance for the development of food or medicine of the polysaccharide.

Materials and methods

Reagents and materials

Chia seeds was purchased from local supermarket (Guayaquil, Ecuador). Chromatographic columns of DEAE Sepharose Fast Flow and Sepharose CL-6B were purchased from GE Healthcare (Chicago, USA) and Saipurusi Technology Co., Ltd. (Beijing, China), respectively. Standard monosaccharides were supplied by Shanghai Yuanye Biological Technology Co., Ltd (China). 1-Phenyl-3-methyl-5-pyrazolone (PMP), trifluoroacetic acid (TFA), pyridine and N-(3-Dimethylaminopropyl)-N-ethyl carbodiimide hydrochloride (CMC) were obtained from Shanghai Baishunyao Biological Technology Co., Ltd (China). Sodium borodeuteride (NaBD_4) and iodomethane (CH_3I) were purchased from Shanghai Xiandong Biotechnology Co., Ltd (China). Thiazolyl blue tetrazolium bromide (MTT), dimethyl sulfoxide (DMSO) and deuterium oxide (D_2O) were purchased from Sigma-Aldrich Chemical Co. (St. Louis, USA). The mouse RAW 264.7 cells were purchased from Tianjin Chuangke Biotechnology Co., Ltd (Tianjing, China). All other chemicals and solvents were analytical grade from Beijing Chemical Co. (Beijing, China).

Extraction of CSP-A

Chia seeds (50 g) was mixed with ultrapure water (1:20, g/mL) under constant stirring for 4 h. The mixture was centrifuged for the first time (8000 rpm, 30 min) in the centrifuge tube, the upper layer was collected, the lower seeds were mixed with ultrapure water again (1:10, g/mL) for 2 h and centrifuged secondly (8000 rpm, 30 min). The above two supernatants were mixed, evaporated and lyophilized, the crude polysaccharides were obtained. The crude polysaccharide was degreased with *n*-hexane, washed with ethanol, acetone and ether for impurity removal, removed by dialysis for small molecular impurities, and freeze-dried to obtain CSP.

Isolation and purification of CSP-A

The crude polysaccharide of CSP was measured and prepared into 1 mg/mL polysaccharide solution. The polysaccharide solution was initially separated by DEAE Sepharose Fast Flow ion-exchange column (3.5 cm × 40 cm), and eluted with 0.1–0.8 M NaCl solution successively at the flow rate of 0.5 mL/min. The elution process was monitored by phenol-sulfuric acid method at 490 nm (5 mL/tube). The eluents were collected and lyophilized to obtain polysaccharides of different components. Polysaccharide solution of 0.3 M NaCl component was prepared into 10 mg/mL, which was purified by Sepharose CL-6B gel filtration column (1.6 cm × 100 cm) and eluted with pure water at the flow rate of 0.5 mL/min. The elution curve was drawn by phenol-sulfuric acid method. All tubes were collected and freeze-dried to obtain white and fluffy homogeneous polysaccharide CSP-A.

Purity text

Polysaccharide samples separated by gel chromatographic column under item 2.3 were obtained and prepared into 5 mg/mL polysaccharide solution with ultra-pure water and 0.22 μm microporous filter membrane. The peak shape and symmetry were observed by HPGC-RI, a series differential refraction detector in Waters University gel liquid chromatograph. Chromatographic conditions: Column: TSK gel-G5000PWXL (7.8 × 300 mm, 5 μm) and TSK gel-G3000PWXL (7.8 × 300 mm, 5 μm) in series; Mobile phase: 0.1 mol/L NaNO₃ solution; Equal elution, flow rate: 0.5 mL/min; Column temperature: 35 °C; Sample size: 20 μL; Detector: 1240 differential refraction detector; BREEZE Software.

Chemical composition analysis

The total sugar content, uronic acid content were determined by phenol-sulfuric acid method, m-hydroxy-biphenyl metho, respectively (Bai et al., 2017; Bornik & Kroh, 2013; Xu, 2019; Blumenkrantz & Asboe-Hansen, 1973; Ren et al., 2018).

Structural characterization

Ultraviolet spectrum analysis and FT-IR spectroscopy analysis

Ultraviolet-Visible spectrum of 1.0 mg/mL CSP-A was recorded in a spectrophotometer (Carry-100, Varian, USA). Fourier-transform infrared (FT-IR) spectrum of CSP-A was carried out at room temperature with the potassium bromide pellet method on Fourier transform-infrared spectrometer (Nicolet, IS50, America).

Molecular weight of CSP-A

The molecular weight of CSP-A were identified by high-performance gel-permeation chromatography (HPGPC). Using the Agilent 1100 High performance Liquid chromatography (HPLC) system, the column was TSK-GEL G5000 PWXL column (7.8 mm × 300 mm) in series TSK-GEL G3000 PWXL column (7.8 mm × 300 mm) equipped with multi-angle laser scattering detector (mall) and refractive index detector (RI). The determination procedure was carried out according to the literature

method (Goh et al., 2016). It was eluted with 0.1 M NaNO₃ solution at 35 °C and a flow rate of 0.5 mL/min. Data was analyzed by ASTRA software. According to the peak shape of the HPGC chromatogram, the homogeneity of CSP-A can be judged. Meanwhile, weight-average molecular weight (Mw), number-average molecular weight (Mn), Z-average molecular weight (Mz), and Z-average radius of gyration (Rz) of the CSP-A were also detected by HPGC-MALLS-RI.

Monosaccharide composition analysis of CSP-A

The monosaccharide composition analysis of CSP-A was performed by using the 1 PMP pre-column derivatization with HPLC. Briefly, 5 mg/mL CSP-A aqueous solution was hydrolyzed with 2 mL 4 M TFA at 120 °C for 4 h in a sealed glass tube. After the hydrolysis completed, dry the above solution up with Nitrogen, add methanol and repeat the above dried procedures five times to remove the excess TFA in the hydrolysis product. Dried hydrolysis product was added into PMP methanol solution for derivatization, and the derivates were analyzed by HPLC. Diamonsil C18 column (4.6 mm × 250 mm) was used with mobile phase consisting of 17 % acetonitrile and 83 % of 0.1 M phosphate buffer (pH = 6.8) at isoelution rate of 1.0 mL/min. The same method was used to detect monosaccharide controls. The monosaccharide composition of CSP-A was determined by chromatographic results of standard sugars (D-glucose, D-mannose, D-galactose, D-galacturonic acid, D-xylose and D-glucuronic acid), and the content of each monosaccharide in CSP-A was calculated by corresponding peak area.

Congo-red assay

The Congo red assay was used to determine whether CSP-A had a helical structure, according to previously reported with slight modifications (Ogawa, Wanatabe, Tsurugi, & Ono, 1972). 0.5 mL 1.0 mg/mL CSP-A solution and 0.5 mL 80 μmol/L Congo red solution were mixed, and the concentration of NaOH in the mixtrue was adjusted to 0.1, 0.2, 0.3, 0.4 and 0.5 mol/L with 1.0 mol/L NaOH solution, and the above sample solutions were kept for 10 min at room temperature and scanned by UV spectrophotometer in the scanning range of 400–600 nm, and the maximum absorption wavelength of every sample was used as the ordinate, and the concentration of NaOH was used as the abscissa to draw a curve.

Circular dichroism spectrum and optical rotation experiment

The Optical rotation of 1.0 mg/mL CSP-A was confirmed using a CDP-001 digital polarimeter (Jahanbin, Abbasian, & Ahang, 2017). Circular dichroism spectrum (CD) of CSP-A refers to the method of Feng et al. with slight adjustments (Feng et al., 2019).

Periodate oxidation and Smith degradation

30.0 mg CSP-A was added into a 25 mL brown volumetric flask, then filled up with 0.015 mol/L NaIO₄ solution, tin foil wrapped, placed in the dark at 4 °C and monitored its absorption at 223 nm every 24 h (0, 24, 48, 72, 96, 120 and 144 h) until its absorbance was constant. The reaction was terminated by ethylene glycol, the consumption amount of periodate was calculated, and the amount of formic acid produced was calculated by the titration with NaOH standard solution. The product of periodate oxidation was placed in a dialysis bag (3500 Da), dialyzed with deionized water for 48 h, lyophilized, reduced by NaBH₄, hydrolyzed by TFA at 120 °C for 4 h, then added 2 mL methanol and dried the solution up with Nitrogen, repeated the above methanol added and dried procedures five times to remove TFA. Later pyridine and acetic anhydride were added and aldononitrile acetate derivatives were obtained and analyzed by GC-MS (Agilent, 7890A-5975C, USA). Standards of glycerin, erythrose, mannose, and xylose were treated as above.

Methylation analysis

To avoid the interference effect of uronic acid on the polysaccharides methylation, the reduction of uronic acid is required. 500 mg carbodiimide was added into 20 mL 1.0 mg/mL CSP-A solution and stirred for

3 h at pH 4.75, and 15 mL 5 mg/mL NaBD₄ solution were added to reduce the uronic acid in the polysaccharide, and the solution was kept stirring for 2 h after the pH was adjusted to 7.0 with 2 M HCl. The above reduction reaction was repeated twice and the reduced polysaccharide was treated by PMP pre-column derivatization, and the contents of glucuronic acid and glucose in the reduced polysaccharide were determined.

Methylation analysis was completed according to the reported method (Jahanbin, Abbasian, & Ahang, 2017). 5.0 mg reduced polysaccharide was dissolved in 5.0 mL DMSO, and 1.5 g methyl sulfonyl sodium was added, then the solution was mixed for 30 min by ultrasound. The above solution was wrapped with tin foil, and 500 ~ 1000 μL CH₃I reagent was added in batches in the dark, and the mixture was stirred for 1 ~ 2 h at a temperature of 17 ~ 30 °C. The reaction was terminated by adding 7 mL H₂O into the reaction system. The methylation products were extracted by chloroform and its IR spectroscopy was analyzed to judge whether the methylation of the reduced polysaccharide was complete by observing whether 3500 cm⁻¹ had an absorption peak.

5 mg/mL methylated polysaccharide solution was hydrolyzed with 2 mL 4 M TFA at 120 °C for 4 h, and TFA evaporated with methanol help, then the hydroxyl in the broken Glycosidic bond of the hydrolysate was labeled and reduced by 20.0 mg NaBD₄ and glacial acetic acid was dropped in the reaction system to remove the excess NaBD₄ until no bubbles emerged, then the solution was dried by evaporation with methanol help, and the dried product was acetylated with 4 mL acetic anhydride / pyridine (1:1, V/V) 3 times to obtain Partially Methylated Alditol Acetate (PMAA), which was extracted with chloroform 3 times and analyzed by GC-MS. The GC-MS (Agilent, 7890A-5975C, USA) was equipped with a DB-5 column (30 m × 0.25 mm, 0.25 μm) programmed from 150 °C to 260 °C at 5 °C /min and 260 °C holding 2 min, then from 260 °C to 280 °C at 10 °C /min.

NMR analysis

30.0 mg CSP-A was dissolved in 1.0 mL Deuteroxide and evaporated to dryness, and the above steps were repeated three times. The sample was detected by nuclear magnetic resonance instrument (Bruker Avance III 600, Germany) to obtain 1D ¹H spectrum and ¹³C spectrum, and 2D ¹H-¹H COSY spectrum and ¹H-¹³C HSQC spectrum.

SEM and AFM analysis of CSP-A

The color and texture of CSP-A were observed, and the microscopic state was observed by scanning electron microscope (SEM). A small amount of dried CSP-A was spread on the conductive adhesive of a circular sample table and gold was sprayed inside the vacuum sprayer for 120 s, and the morphology of CSP-A was observed under a scanning electron microscope (JEOL, JEM-6700F, Japan). The CSP-A was detected and analyzed by atomic force microscopy (Bruker, Dimension FastScan Bio, Germany) to obtain the AFM map, amplitude error map and 3D-AFM map of CSP-A.

Antioxidant activities of CSP-A

DPPH scavenging activity

1 mL CSP-A solution with different concentrations (0.25, 0.5, 1, 2 and 4 mg/mL) was mixed with 1 mL 100 μmol/mL DPPH ethanol solution, respectively. Shake well and react at room temperature for 30 min away from light. Absorbance is measured at 517 nm. The above experiments were carried out with vitamin C as positive control. All tests were performed in triplicate. DPPH· scavenging rate was calculated as follows:

$$\text{DPPH· scavenging rate (\%)} = [1 - (A_1 - A_0)/A_2] \times 100\% \quad (1)$$

Where A₀ is the absorbance of the CSP-A solution without DPPH, A₁ is the absorbance of the CSP-A and DPPH·-mixture solution, A₂ is the

absorbance of the DPPH solution without CSP-A.

OH scavenging activity

OH radical scavenging activity of CSP-A was assessed according to the following operation. Briefly, 50 μ L 2.25 mmol/L FeSO₄ aqueous solution, 50 μ L 9 mmol/L salicylic acid methanol solution, 50 μ L a serials of concentrations CSP-A solution (0.25, 0.5, 1, 2 and 4 mg/mL) and 50 μ L 8.8 mmol/L H₂O₂ solution were added into the centrifuge tube. The reaction was incubated at 37 °C for 30 min, and the absorbance value was measured at 510 nm by microplate reader. Vitamin C was used as a positive control and performed the experiments described above. All tests were performed in triplicate. OH scavenging rate was calculated according to the following formula:

$$\text{OH-scavenging rate (\%)} = [(A_2 - A_1)/(A_0 - A_1)] \times 100\% \quad (2)$$

Where A₀ was the absorbance of the blank solution in which CSP-A and H₂O₂ were replaced with ultrapure water, A₁ was the absorbance of the control solution without CSP-A, A₂ was the absorbance of the sample solution.

Immunomodulatory activity of CSP-A

Cell viability assay

Cryopreserved RAW 264.7 cells were resuscitated, passaged and cultured for the polysaccharide immunoactivity assay. RAW 264.7 cells viability was determined according to the previous method (Zhang et al., 2019). RAW 264.7 cells in logarithmic growth phase were seeded in 96-well plates at a density of 1000 cells/well, and incubated in a cell culture box for 24 h, and 500 μ L 6.25 ~ 100 μ g/mL different concentrations CSP-A in the cell culture medium were respectively added into the above cells wells as the experimental group, and the blank control group was given the same volume cell culture medium without CSP-A, and the culture medium was removed after incubated continuously for 24 h, and 10 μ L 10 mg/mL MTT reagent was added into each well, and then incubated at 37 °C for 4 h. The above culture medium was carefully discarded, and 100 μ L DMSO was added into each well and shaken on a shaker for 10 min to fully dissolve the formazan, a blue-purple crystal. The optical densities (OD values) were measured at 490 nm, and cell proliferation activity was calculated according to the following formula:

$$\text{Cell proliferation activity (\%)} = (\text{OD}_{\text{sample}}/\text{OD}_{\text{control}}) \times 100\% \quad (3)$$

Phagocytosis assay

Neutral red phagocytosis assay was used to evaluate the phagocytic activity of CSP-A on RAW 264.7 cells. RAW 264.7 cells in logarithmic growth phase were seeded into 96-well plates at 5×10^4 cells /well and incubated for 24 h. In the experimental groups, 500 μ L 6.25, 12.5, 25 and 50 μ g/mL CSP-A solutions were respectively added and cultured in 5 % CO₂ and 37 °C culture box for 48 h. 5 μ g/mL LPS was used as the positive control group, and the culture medium instead of CSP-A solutions was used as the blank control group. The culture medium was discarded, and 100 μ L 0.1 % neutral red solution was added into each well and incubated continuously for 1 h. The supernatant was discarded and eluted the cells three times with 0.01 M PBS to remove neutral red that was not engulfed. Then 200 μ L cell lysate (ethyl alcohol:0.01 % acetic acid = 1:1) was added into each well and left at 4 °C overnight. The OD value of each well was measured at the wavelength of 540 nm, and the cell phagocytosis rate was calculated according to the following formula:

$$\text{Cell phagocytosis rate (\%)} = (\text{OD}_{\text{sample}}/\text{OD}_{\text{control}}) \times 100\% \quad (4)$$

NO release assay

Macrophages in the logarithmic growth phase were collected, the cell density was adjusted to 5×10^5 cells /well, and incubated for 24 h at 37 °C. The culture medium was discarded and DMEM culture medium

was added. 500 μ L 25, 50 and 100 μ g/mL CSP-A solutions were respectively added into each well as the experimental groups, 5 μ g/mL LPS was used as the positive control group, and the culture medium instead of CSP-A solution was used as the blank control group, and the above solutions groups were cultured at 37 °C for 24 h. At the end of the culture, the cell culture medium in the well was transferred into a centrifuge tube, centrifuged at 2500 r/min for 5 min, and the supernatant was collected. According to the nitric oxide (NO) detection kit method, the content of NO in the supernatant was calculated with the measured standard curve of NO.

Cytokine secretion assay

The levels of TNF- α , IL-6 and IL-1 β were determined according to the previous reports (Tabarsa et al., 2019). RAW 264.7 cells in logarithmic growth phase were used to adjust the cell concentration to 3×10^5 cells/well and incubated for 24 h at 37 °C. RAW 264.7 cells were incubated with 500 μ L different concentrations CSP-A (25, 50 and 100 μ g/mL) for 24 h, and the supernatants were collected. The release of TNF- α , IL- α and IL-1 β was detected by ELISA kit. The culture medium instead of 500 μ L CSP-A solution was used as a blank control group.

Statistical analysis

Each experiment was repeated at least three times. All data are presented as mean \pm SD analyzed by Graphpad prism 7.0 software, and the statistical significance was evaluated by one-way ANOVA. P < 0.05 was considered statistically significant.

Results and discussions

Extraction, isolation and purification of CSP-A

The extraction and separation method adopted is slightly modified based on the method of Timilsena et al. (2016) 0.362 g crude chia seeds polysaccharides were extracted from 50.0 g chia seeds by water extraction and centrifugation, and 1.52 g total chia seeds polysaccharides were obtained from crude chia seeds polysaccharides by degrease, alcohol precipitation, deproteinization and dialysis. The total chia seeds polysaccharides were named briefly CSP after removed the impurities. The purified CSP were loaded on a DEAE FF ion-exchanged column, eluted with 0.1 ~ 0.8 M NaCl and detected with phenol-sulfuric acid method. The elution curve of the DEAE FF ion-exchange chromatographic curve is shown in Fig. 1A, and the polysaccharides fraction of 0.3 M NaCl was collected. Further purification was performed on a Sepharose CL-6B column in order to obtain highly purified polysaccharides for structural characterization and activity assessment. The gel chromatographic elution curve of the 0.3 M NaCl polysaccharides fraction is shown in Fig. 1B, tubes 22 to 36 were collected, concentrated by rotary evaporation, freeze-dried and named CSP-A.

Purity test and chemical composition analysis

The chromatographic diagram of CSP-A gel separated and purified by DEAE FF and Sepharose CL-6B columns is shown in Fig. 1D. The peak shape of HPGPC-RI chromatogram is symmetrical and simple, and the polysaccharide can be considered as pure polysaccharide with uniform molecular weight distribution. In addition, the total sugar content of CSP-A was 35.92 % and the uronic acid content was 60.11 %. The protein content determination results are too small to be ignored. Timilsena and Goh et al. determined that the protein content of total polysaccharide of chia seed after impurity removal was 2.6 % and 3.8 %, respectively, indicating that the addition of acetone in the process of impurity removal had a high protein removal efficiency, but a small amount of binding protein was difficult to remove even with the addition of organic reagents.

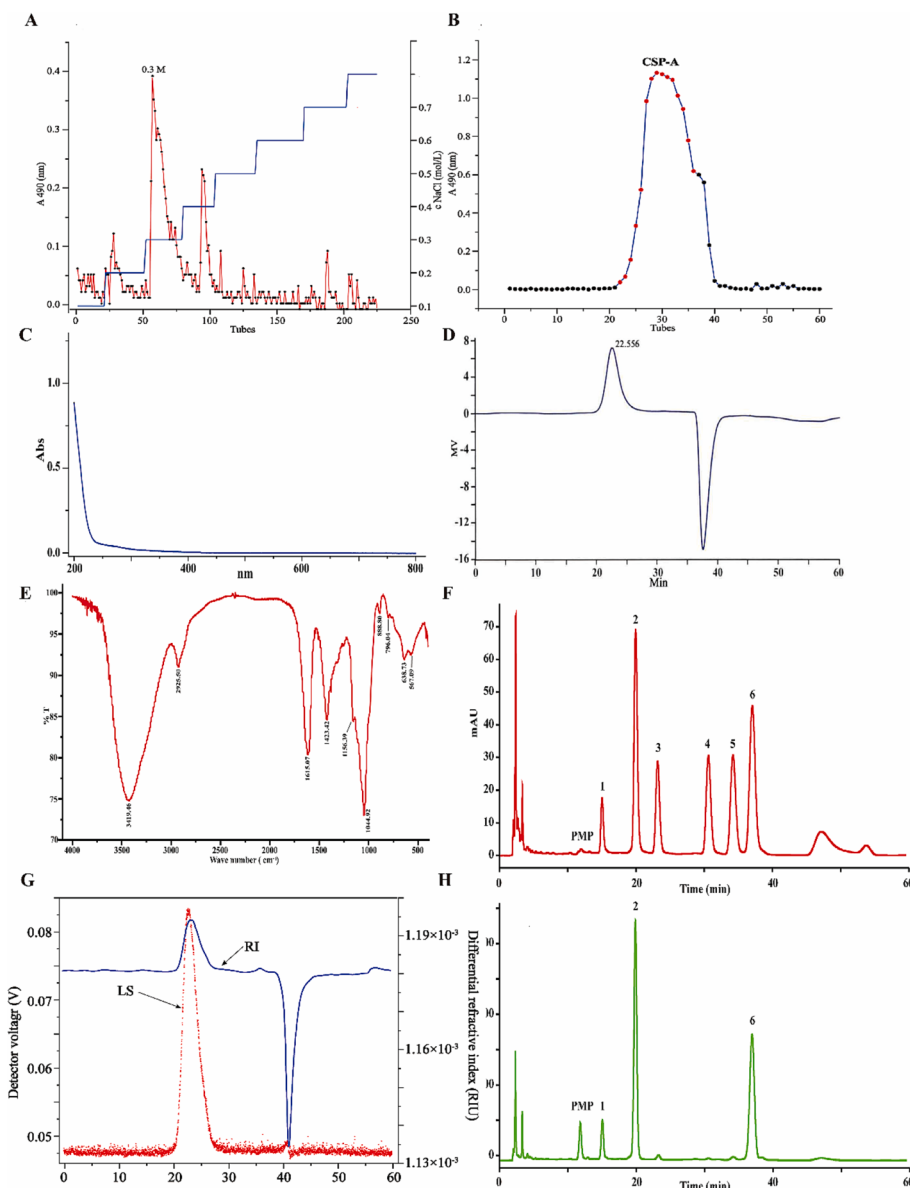


Fig. 1. Elution curves of CSP-A on DEAE FF column (A) and Sepharose CL-6B column (B); UV spectrum of CSP-A (C); Chromatogram of HPGC-RI purity test for CSP-A (D); FT-IR spectrum of CSP-A (E); HPGC-MALLS-RI profile of CSP-A(G); HPLC chromatograms of PMP derivatives of 6 standard monosaccharides (1. Mannose. 2. glucuronic acid; 3. galacturonic acid; 4. glucose; 5. galactose; 6. xylose) (F) and monosaccharide composition of CSP-A (H).

Structural characterization

Ultraviolet spectrum analysis

There was a strong absorption at 200 nm and no strong absorption peak at 260 ~ 280 nm in the UV spectrum of CSP-A solution (Fig. 1C), indicating that there was no nucleic acid and free protein in the CSP-A sample. But there may be very few binding proteins (Lu et al., 2019).

FT-IR spectroscopy analysis

The relative configuration of glycosidic bonds can be determined according to the bending vibration of the C—H bond of the sugar terminal group in FT-IR spectrum. The absorption peak at $844 \pm 8 \text{ cm}^{-1}$ was judged as the α anomer, and the absorption peak at $891 \pm 7 \text{ cm}^{-1}$ was judged as the β anomer. In the FT-IR spectrum of CSP-A (Fig. 1E), CSP-A had an absorption peak at 888.80 cm^{-1} , indicating the existence of β -configuration glycosidic bond. The intense peak at 1044.92 cm^{-1} represented the C—O—C stretching vibration. The peak between 1160 and 1045 cm^{-1} was assigned to the stretching vibration of C—O—C and

the bending vibration of C—O—H in the glycoside, indicating that a complete sugar ring structure exists (Zhou et al., 2020). The intense characteristic peak at 3419.46 cm^{-1} represented the O—H stretching vibration of the backbone structure of saccharide chain. The weak absorption peak at 2925.50 cm^{-1} was attributed to the C—H stretching vibration on the aromatic ring and methyl group. Similar to the infrared spectrum of chia seed polysaccharide reported by Goh et al. (Goh et al., 2016), the absorption peak at 1615 cm^{-1} was attributed to the stretching vibration peak of the mannose ring.

Molecular weight of CSP-A

The chromatographic behavior of CSP-A was detected by HPGC-MALLS-RI, as shown in Fig. 1G, the chromatogram of CSP-A showed symmetrical and single peak, indicating that CSP-A was a homogeneous polysaccharide with uniform molecular weight distribution and could be used for further structural and biological activity studies. As shown in Table S1, Mw/Mn or Mz/Mn of CSP-A approached 1.0, which indicated a narrow molecular mass distribution of the homogeneous

polysaccharide, and Mw of CSP-A was 1.688×10^5 Da and Rz was 41.2 nm, in which Mw/Mn and Rz are close to the reference (Goh et al., 2016). Timilsena et al. (Timilsena et al., 2016) used high performance gel chromatography combined with standard glucan curve to detect the Mw of pure polysaccharide of Chia seeds as 2.3×10^6 Da. Goh et al. (Goh et al., 2016) used HPLC-MALLS-RI technology to detect the molecular weight parameters of chia seed polysaccharide, and obtained Mw = 4.9×10^5 Da, Rz = 39 nm, and Mw/Mn = 1.02, among which the data of Rz and Mw/Mn were not significantly different from those in this paper, which proved the reliability of this method.

Monosaccharide composition analysis

The monosaccharide composition of CSP-A was investigated by PMP pre-column derivatizations, and the monosaccharide composition chromatograms of mixed monosaccharide standard and CSP-A are shown in Fig. 3 (Fig. 1F and Fig. 1H). There might exist a very small amount of galactose or galacturonic acid while D-mannose, D-glucuronic acid and D-xylose were confirmed in CSP-A. Only considering the 3 large amounts of monosaccharides, which were D-mannose, D-glucuronic acid and D-xylose, CSP-A was a heteropolysaccharide composed of D-mannose, D-glucuronic acid and D-xylose in the molar ratio of 1:3:4. In addition, Timilsena et al. (2016) studied that the monosaccharides in chia seed polysaccharide mainly consisted of glucuronic acid, galacturonic acid, arabinose, glucose, galactose and xylose, among which xylose and glucose accounted for the largest proportion, the ratio was close to 2:1. Goh et al. (2016) tested chia seed polysaccharide by GC and HPLC, which was mainly composed of glucose, galactose, arabinose, mannose and xylose, with glucose accounting for up to 80 %. Different studies have found that the monosaccharide composition and proportion of homogeneous polysaccharide from chia seeds are different, which may be related to the origin and genetic variety of chia seeds, the extraction and purified conditions to obtain the homogeneous polysaccharide.

Congo-red assay

Congo red reagent can form a complex with a polysaccharide solution with a helical chain conformation. The maximum absorption wavelength of the complex is redshifted, and when the alkaline concentration reaches a certain value, the maximum absorption wavelength decreases sharply. As shown in Fig. 2A, when the concentration of NaOH increased from 0 to 0.4 M, the maximum absorption wavelength of the complex formed by and CSP-A increased from 498 nm to 516 nm and was red-shift compared to the blank Congo red reagent, indicating that CSP-A formed a regular helical structure (Hui et al., 2019). When the concentration of NaOH was increased to 0.5 M, the maximum absorption wavelength of the complex decreased to 512 nm, indicating that the helical structure of CSP-A began to decompose into an irregular linear structure (Xu et al., 2018). It was concluded that the molecule of CSP-A might be a helix structure in aqueous solution, but its other spatial conformation, such as the number of residues per helical turn and the axial rese between two adjacent units, needs to be further studied. This

research result is consistent with the report of Saito et al. (1991), which believes that only biological macromolecules with high molecular weight (>90 kDa) can form the three-strand helical structure.

Circular dichroism spectrum and optical rotation experiment

The value of optical rotation of CSP-A was $+180^\circ$, indicating the existence of α -glycosidic bond configuration in CSP-A. CD spectra was used to analyze the local ring structure near the carboxyl group on its molecular chain and the configuration change of asymmetric saccharide in solution according to the change of optical rotation of the sample. A positive Cotton effect of CSP-A appears near 198 nm, and a strong negative Cotton effect appears near 210 nm (Fig. 2B), indicating that CSP-A contained much glycuronic acid and existed in an asymmetric form in aqueous solution. The main reason is that polysaccharide samples contain more uronic acid, and the CD spectrum curve of polysaccharide is related to the local ring structure near the carboxyl group on the molecular chain (Zhu et al., 2014).

Periodate oxidation and Smith degradation

Periodate oxidation played an auxiliary role in confirming the structural information of the polysaccharide. 1 mol of CSP-A hexose residue consumed 1.406 mol of periodate and yield formic acid. The formation of formic acid was detected in the oxidation of periodate, indicating that there was $(1 \rightarrow)$ or $(1 \rightarrow 6)$ glycosidic bonds in CSP-A. There was $(1 \rightarrow)$ or $(1 \rightarrow 6)$ or $(1 \rightarrow 2)$ glycosidic bonds in $-\text{GlcA}-$ or $-\text{Manp}-$ to yield glycerol after Smith degradation, or $(1 \rightarrow 4)$ glycosidic bonds in $-\text{Xylp}-$ to yield glycerol and glycol after Smith degradation. There might also be unoxidized glycosidic bonds in CSP-A, namely $(1 \rightarrow 3)$ and $(1 \rightarrow 2,4)$ bonds.

Based on the difference between the products before and after Periodate oxidation and Smith degradation, GC-MS were used to preliminarily infer the linkage position of glycosidic bonds in CSP-A (Abdel et al., 1952). As shown in Fig. 3A and Fig. 3B, erythritol was not detected in CSP-A sample, which indicated that there was no $(1 \rightarrow 4)$ glycosidic linkages in $-\text{GlcA}-$ or $-\text{Manp}-$ and there might existed $(1 \rightarrow 4)$ glycosidic linkages in $-\text{Xylp}-$. Glycerol was detected ($t_R = 23.245$ min), indicating that CSP-A contained $(1 \rightarrow)$, $(1 \rightarrow 6)$, $(1 \rightarrow 2)$ or $(1 \rightarrow 2,6)$ glycosidic linkages $-\text{GlcA}-$ or $-\text{Manp}-$. Xylose was detected ($t_R = 33.115$ min), indicating that the xylose junction sites might be $(1 \rightarrow 3)$, $(1 \rightarrow 2,3)$, $(1 \rightarrow 2,4)$, $(1 \rightarrow 3,4)$ or $(1 \rightarrow 2,3,4)$.

Methylation analysis

Methylation analysis is an indispensable experimental means to determine the junction sites of sugar residues in the polysaccharide. The difference between gas chromatogram of unreduced and reduced CSP-A was the significant increase of the peak area of peak 2 (Fig. 3C and 3D), which proved that peak 2 was the peak of methylated glucose acetate derivative after the esterification and reduction of glucuronic acid residues, and the connection site of glucuronic acid residues could be determined by the connection site of glucose. The methylated GC-MS ion fragments of CSP-A are shown in Fig. 3E-H. The connection

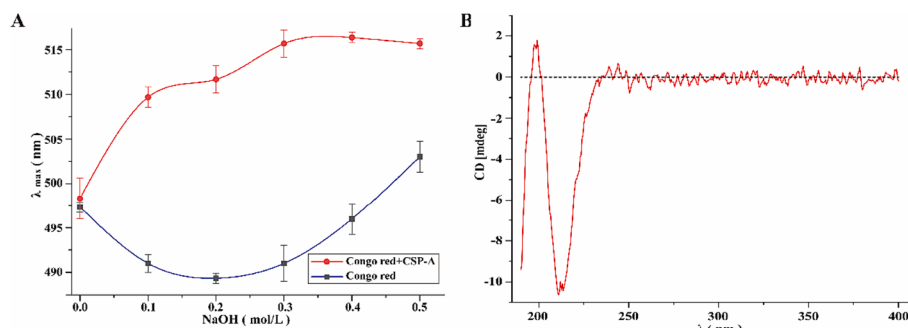


Fig. 2. Maximum absorption wavelengths of Congo red and its complex at different NaOH concentrations (A); CD spectrum of CSP-A(B).

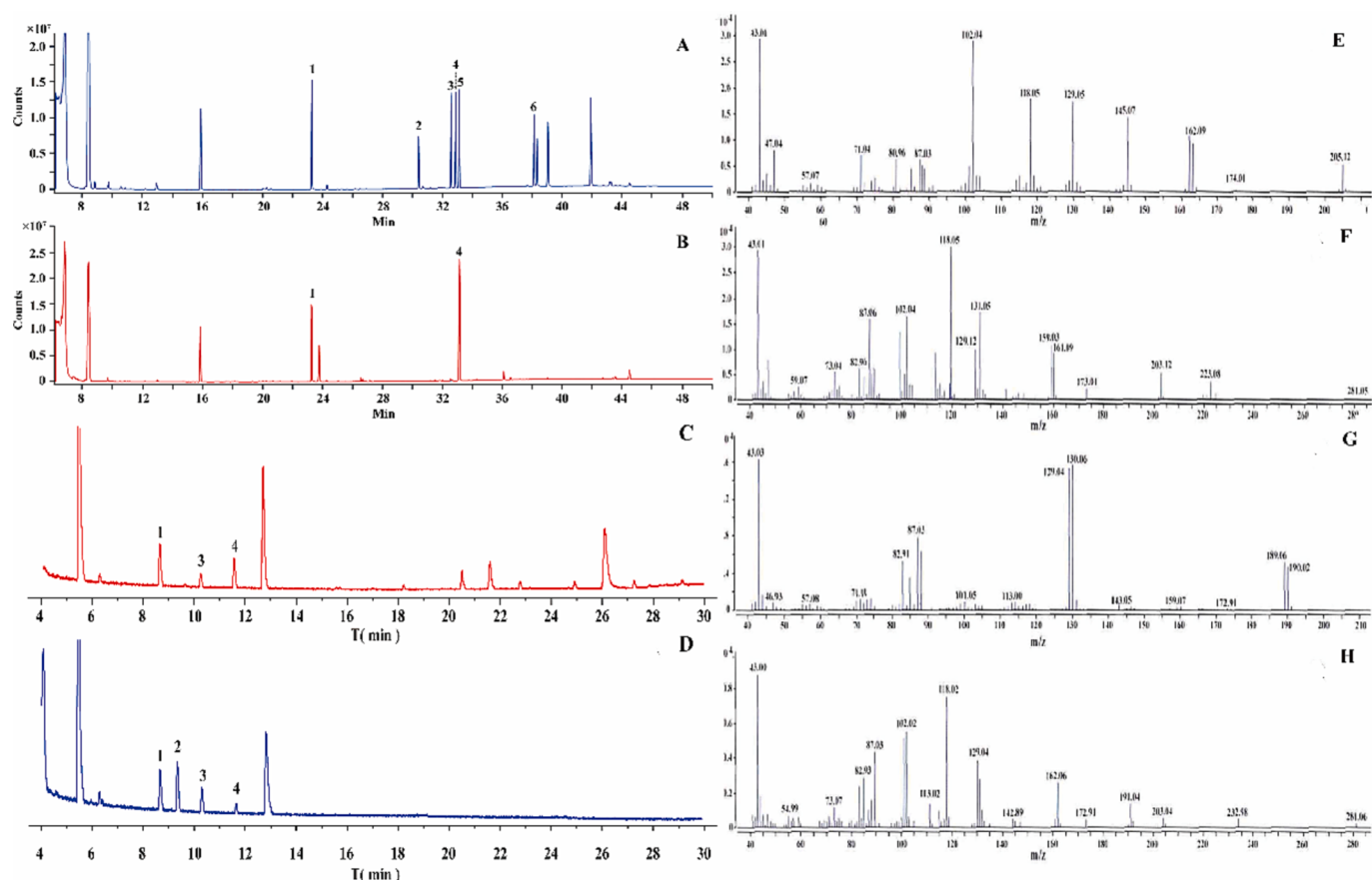


Fig. 3. GC-MS chromatograph of products after Smith degradation(A) mixed standard (1: glycerol; 2: erythritol; 3: rhamnose; 4: xylose; 5: arabinose; 6: mannose) and (B) CSP-A; GC-MS chromatograms of unreduced CSP-A (C) and esterified reduced CSP-A (D); Chia seed polysaccharides CSP-A methylated GC-MS ion fragments (E: d-Manp-(1→, →6)-d-GlcpA-(1→; G: →2,4)-d-Xylp-(1→; H: →6)-d-Manp-(1→).

positions of major monosaccharide residues in CSP-A were determined through comparing the major fragment ions of PMAA (Table S2) with relevant literature data and the EI-MS Spectral Database for PMAA's from the Complex Carbohydrate Research Center (CCRC) at the University of Georgia (<https://www.ccrc.uga.edu/>). According to the EI-MS Spectral Database for PMAA's, there were 4 kinds of sugar residues in CSP-A, which respectively were d-Manp-(1→, →6)-d-GlcpA-(1→, →2,4)-d-Xylp-(1→ and →6)-d-Manp-(1→. The linkage position of d-xylose was →2,4)-d-Xylp-(1→, consistent with the conclusion that xylose was detected in the Smith degradation experiment, and the linkage position of d-mannose had terminal connection, consistent with the conclusion that glycerol was detected in the Smith degradation.

NMR analysis

NMR analysis can be used to obtain structural information such as the relative configuration of end-group carbon and end-group hydrogen and the joining order of sugar residues. Combined with the results of methylation analysis, the structure of the polysaccharide can be further obtained. ^1H NMR signals of CSP-A were mostly in the range of 3.1–5.3 ppm, and the terminal hydrogen signals were in the range of 4.5–5.5 ppm (Fig. 4A). The terminal hydrogen signals of 5.22 and 4.55 ppm (Fig. 4A) were respectively assigned to α and β configurations of glycosidic bond. The terminal hydrogen signal of CSP-A also overlapped with the strong signal of the D_2O solvent. The spectral peaks between 3.1 and 4.5 ppm were the signals stacking from the protons on the C-2, C-3, C-4, C-5, and C-6 of the sugar ring. Consistent with the ^1H NMR spectrum of chia seeds polysaccharide studied by Timilsena et al. (Timilsena et al., 2016), there were hydrogen signal peaks at 1.2, 1.8 and 1.9 ppm, which could be attributed to the hydrogen signal peaks of CH_3 at C- CH_3

or COOCH_3 . The ^{13}C NMR spectrum (Fig. 4B) showed that the carbon signal of CSP-A was mostly distributed between 60 and 180 ppm, and the absorption peak at 177.09 ppm could be attributed to the C-6 carbonyl signal in glucuronic acid, which was consistent with glucuronic acid detected in CSP-A and it was also consistent with the conclusion of 176.9 ppm of the ^{13}C NMR spectrum of the kia-seed polysaccharide (Timilsena et al., 2016). The chemical shift between 95 and 105 ppm was the signal of the glycan terminal carbon. Four terminal carbon signals of 97.69, 97.71, 101.38 and 101.81 ppm were detected. The chemical shift between 60 and 85 ppm was the carbon signal from C-2 to C-6 on the sugar ring.

The sugar residues d-Manp-(1→, →6)-d-GlcpA-(1→, →2,4)-d-Xylp-(1→ and →6)-d-Manp-(1→ obtained by methylation analysis were labeled as A, B, C, and D, respectively. In the HSQC spectrum of CSP-A (Fig. 4D), and a total of four signals was detected. According to the methylation analysis results, the proportion of →6)-d-GlcpA-(1→ was the largest and the signal was strongest at 5.22 ppm in ^1H NMR and 97.69 ppm in ^{13}C NMR. Combined with the previous data (Timilsena et al., 2016, Lin et al., 1994, Nep & Conway, 2010), the signal of terminal hydrogen and terminal carbon at $^1\text{H}/^{13}\text{C}$ 5.22/97.69, labelled as B, was deduced to be →6)- α -d-GlcpA-(1→. Similarly, in the methylation analysis, the proportion of →6)- β -d-Manp-(1→ was the smallest, and the signal at $^1\text{H}/^{13}\text{C}$ 4.78/101.81 was the weakest compared with the other three signals in the HSQC spectrum. Combined with the literature data (Wu et al., 2020, Yuge et al., 2014), it was inferred that $^1\text{H}/^{13}\text{C}$ 4.78/101.38 was the terminal hydrogen and terminal carbon signals corresponding to →6)- β -d-Manp-(1→ (D). The $^1\text{H}/^{13}\text{C}$ 4.76/97.71 and $^1\text{H}/^{13}\text{C}$ 4.55/101.81 were inferred to be the terminal hydrogen and terminal carbon signals corresponding to β -d-Manp-(1→ (A) (Kuang et al., 2020, Zhang

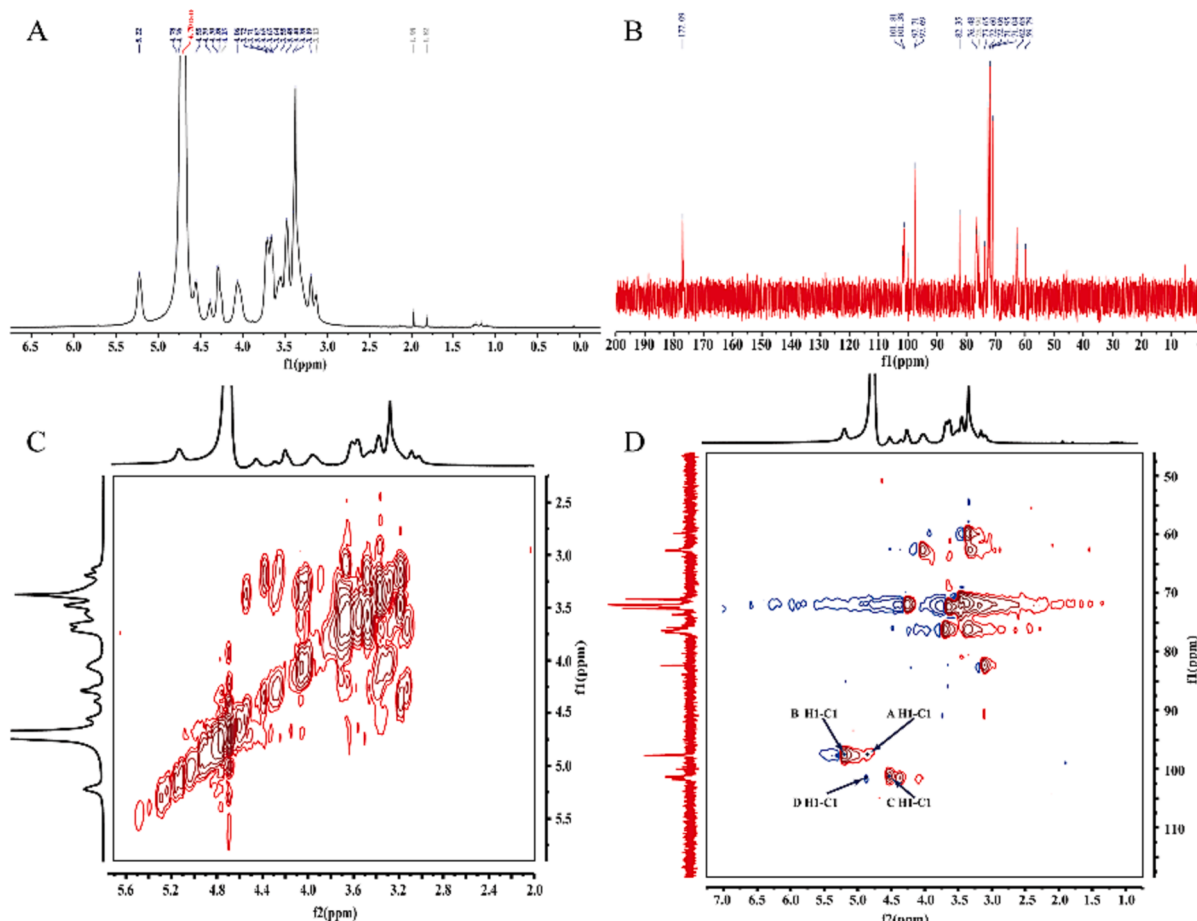


Fig. 4. NMR analysis of CSP-A. (A) The ^1H NMR spectrum (D_2O , 600 MHz) of CSP-A. (B) The ^{13}C NMR spectrum (150 MHz) of CSP-A. (C) The ^1H - ^1H COSY spectrum of CSP-A. (D) The HSQC spectrum of CSP-A.

et al., 2019) and \rightarrow 2,4) $-\beta\text{-D-Xylp}$ -(1 \rightarrow (C)(Chen et al., 2020), respectively.

According to Carbohydrate Structure Database from CCRC at the University of Georgia (<https://www.ccrc.uga.edu/>), the ^1H NMR and $^{13}\text{CNMR}$ signals for the above 4 sugar residues were simulated, and the simulated chemical shifts were entered to search the experimental NMR signals, i.e. the experimental $^{13}\text{CNMR}$ signals of $\beta\text{-D-Manp}$ -(1 \rightarrow (Kohno et al., 1999) and \rightarrow 6) $-\beta\text{-D-Manp}$ -(1 \rightarrow (Ganter et al., 1995) \rightarrow 4)- $\alpha\text{-D-GlcpA}$ -(1 \rightarrow (McNally et al., 2007) and $\beta\text{-D-Xylp}$ -(1 \rightarrow (Shimoyama et al., 2021) were gotten. Compared with the experimental $^{13}\text{CNMR}$ signals of \rightarrow 4)- $\alpha\text{-D-GlcpA}$ -(1 \rightarrow , the chemical shift for C-4 in \rightarrow 6)- $\alpha\text{-D-GlcpA}$ -(1 \rightarrow moved towards higher field and the chemical shift for C-6 in this sugar residue moved 3 ~ 10 ppm towards lower field. \rightarrow 2,4) $-\beta\text{-D-Xylp}$ -(1 \rightarrow had more glycosylated carbon than $\beta\text{-D-Xylp}$ -(1 \rightarrow , the chemical shifts for C-2 and C-4 in \rightarrow 2,4) $-\beta\text{-D-Xylp}$ -(1 \rightarrow both moved towards lower field. Similarly, ^1H NMR signals of \rightarrow 6)- $\alpha\text{-D-GlcpA}$ -(1 \rightarrow (Bystrøva et al., 2000), ^1H NMR signals of $\beta\text{-D-Manp}$ -(1 \rightarrow and \rightarrow 6) $-\beta\text{-D-Manp}$ -(1 \rightarrow (Vinogradov et al., 2002), ^1H NMR signals of \rightarrow 4)- $\beta\text{-D-Xylp}$ -(1 \rightarrow (Castric et al., 2001) were compared with ^1H NMR signals of CSP-A. The chemical shift assignment to ^1H and ^{13}C (Fig. 4A and B) of the above 4 sugar residues was inferred (Table S3).

SEM and AFM analysis of CSP-A

The microstructure of CSP-A was shown in Fig. 5 D-G, CSP-A appeared as coiled aggregates and stacked each other under the microscope of 100 (Fig. 5D) and 200 magnification (Fig. 5E). The surface of CSP-A was relatively compact, and there was irregular branch (Fig. 5F), indicating that CSP-A was an amorphous structure. Under the microscope of 1000 magnification, the surface of CSP-A could be seen to be

relatively smooth (Fig. 5G). Goh et al. observed the fiber structure of scattered clusters of chia seed polysaccharide under SEM, and believed that the fiber structure of these scattered clusters might be protein components, while the polysaccharide showed a rectangular chain structure. Capitani et al. observed under SEM that chia seed gel had a fibrous appearance.

AFM was used to observe the microscopic morphology of CSP-A in the aqueous solution (Fig. 5A and C). There were irregular aggregates and dispersions in the AFM graph of CSP-A, indicating that CSP-A might exist in the form of spherical chain conformation in aqueous solution. This might be related to the presence of intramolecular and intermolecular hydrogen bonds, and the negative charge from glycuronic acid groups of CSP-A. As shown in Fig. 5C, it could be seen that the polysaccharide molecules formed surface protrusions of different heights in aqueous solution, the polysaccharide molecules were relatively dispersed, and the diameter of the aggregates ranged from 33.88 nm to 381.74 nm, and the height ranged from 0 to 2.8 nN in the aqueous solution.

Antioxidant activities of CSP-A

Fig. 6 shows the DPPH- and OH scavenging ability of CSP, CSP-A and Vc. With the concentration increase of CSP-A, the DPPH scavenging rate of CSP-A was gradually enhanced before its concentration reached 2.0 mg/mL, CSP-A showed the strongest DPPH- scavenging activity and the DPPH- scavenging rates of CSP-A was 74.07 % when its concentration was between 2.0 mg/mL and 4.0 mg/mL, then its DPPH scavenging rates decreased when its concentration was over 4.0 mg/mL (Fig. 6A). In the concentration range of 0.25 to 4.0 mg/mL, the OH-scavenging rates of

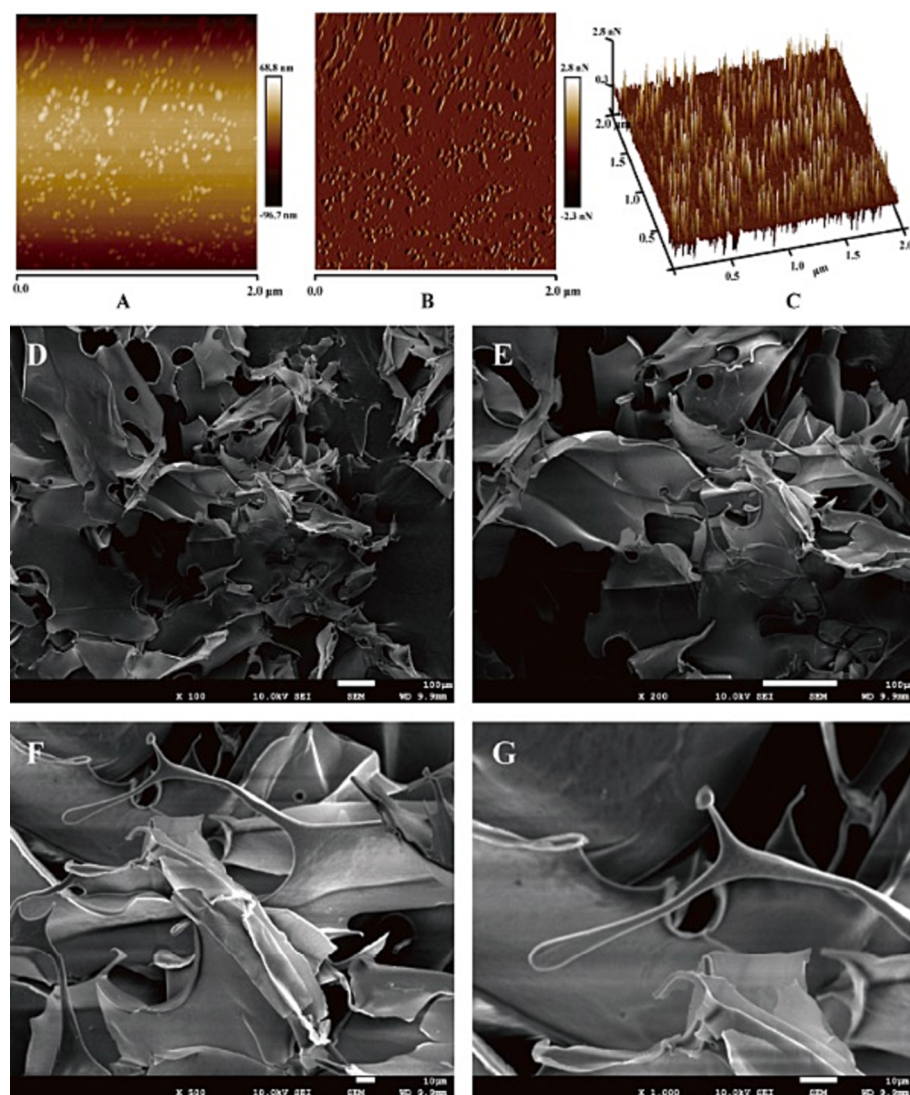


Fig. 5. Microstructure observation of CSP-A. AFM (The scanning range is 2.0 μm): (A) Planar pattern of AFM. (B) Amplitude error pattern of AFM. (C) Stereograph of the AFM. SEM: (D) 100 \times magnification. (E) 200 \times magnification. (F) 500 \times magnification. (G) 1000 \times magnification.

CSP-A showed a dose-dependent increase and reached 60.13 % when its concentration was 4.0 mg/mL (Fig. 6B). The results of the DPPH- and OH-scavenging activity experiments showed that both CSP-A and CSP had antioxidant activity, while they only had moderate ability to scavenge the above two free radicals when compared with Vc, indicating that chia seeds polysaccharide had potential antioxidant effect. In addition, studies have found that chia seeds extract has obvious antioxidant activity and can be used as a potential antioxidant (Uribe et al., 2011). Marineli et al. confirmed the free radical scavenging activity of Chia seeds alcohol extract in vitro (Marineli et al., 2015).

Immunomodulatory activity of CSP-A

Cell viability assay

Macrophages play a crucial role in the immune response, and LPS-induced RAW 264.7 macrophages are commonly used to evaluate the immunomodulatory activity of natural polysaccharides (Jia et al., 2015). A series of 6.25–100 $\mu\text{g}/\text{mL}$ CSP-A concentrations of CSP-A were used to stimulate RAW 264.7 cells to evaluate the cytotoxicity of CSP-A on macrophages RAW 264.7 cells. As shown in Fig. 6C, CSP-A had no effect on the viability of RAW 264.7 cells compared to the control group and had no cytotoxic effect on macrophages in this concentration range.

Therefore, a concentration range of 6.25–100 $\mu\text{g}/\text{mL}$ was selected for subsequent immunoactivity evaluation experiments.

Phagocytosis assay

Phagocytosis activity of macrophages is the primary and basic immune response, the first and necessary defense line of immune response, and an important parameter to evaluate immune activity. Phagocytic capacity is an important index to evaluate the immunostimulatory activity of polysaccharides, and the neutral red assay was used to evaluate the effect of CSP-A on the phagocytic activity of RAW 264.7 cells. Compared with the blank control group, the phagocytosis of macrophages was significantly enhanced by CSP-A, and CSP-A enhanced the phagocytosis rate of macrophages in a dose-dependent manner at the concentration range of 6.25 to 50.0 $\mu\text{g}/\text{mL}$ (Fig. 6D).

NO release assay and cytokine secretion assay

TNF- α , IL-1 β , and IL-6 are important regulators in the immune system, and TNF- α promotes tumor cell death by killing T cells or other cells. IL-1 β and IL-6 play key roles in immune response and protein synthesis in the acute phase (Naugler & Karin, 2008; Castell et al., 1989). As shown in Fig. 6E ~ H, the release amount of NO or different cytokines from RAW 264.7 cells stimulated by 25, 50 or 100 $\mu\text{g}/\text{mL}$ CSP-

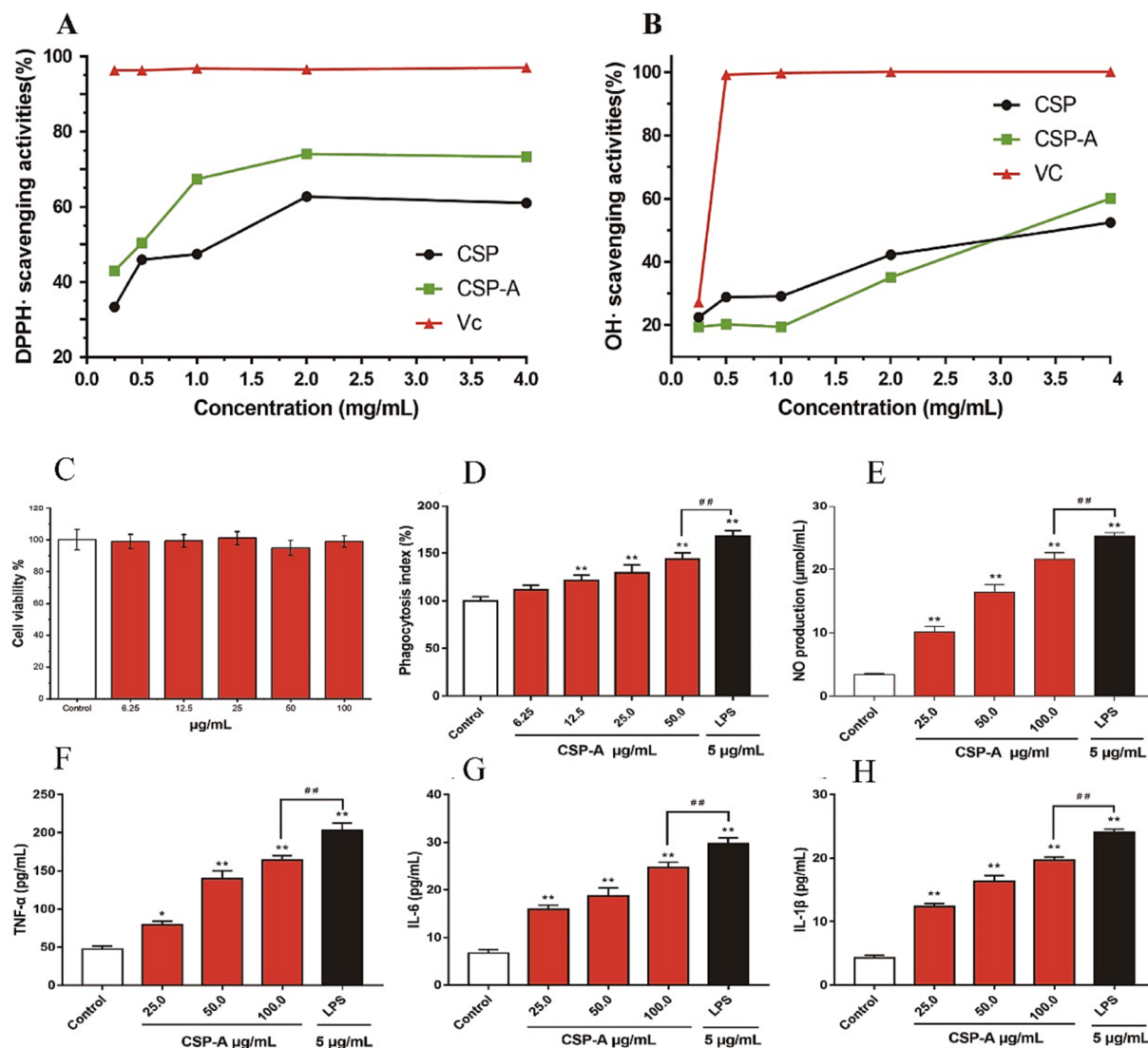


Fig. 6. In vitro antioxidant activity of CSP-A. (A) DPPH[·] scavenging activity. (B) OH[·] scavenging activity; Effects of CSP-A and positive control (LPS) on RAW264.7 cells. (C) Cell viability. (D) Phagocytic activity. (E) NO production. (F) TNF- α levels. (G) IL-6 levels. (H) IL-1 β levels. All values are presented as the mean \pm SD of six independent experiments. *P < 0.01, **P < 0.001 versus the control group; #P < 0.05, ##P < 0.01 versus the LPS group.

A was respectively enhanced compared with the blank control groups (P < 0.01 or P < 0.001), and the secretion of NO, TNF- α , IL-6 and IL-1 β increased in a CSP-A concentration-dependent manner, while the release amount was respectively significantly less than that stimulated by 5.0 μ g/mL lipopolysaccharide (P < 0.01), which indicated that CSP-A could moderately stimulate RAW 264.7 macrophages to secrete NO and pro-inflammatory factors, indicating that CSP-A was involved in cellular immune regulation.

Conclusions

In this study, an acidic heteropolysaccharide CSP-A that had never been studied was extracted from chia seeds, and its basic properties and structures were characterized, and it was determined that CSP-A is composed of mannose, glucuronic acid and xylose, and has β -D-Manp-(1 \rightarrow , -4)- α -D-GlcA-(1 \rightarrow , -2,4)- β -D-Xylp-(1 \rightarrow , and -4)- β -D-Manp-(1 \rightarrow glycosidic bonds. DPPH and OH methods were used to verify that CSP-A has antioxidant activity, in addition, it also has a certain immune promoting effect, stimulates RAW264.7 to enhance phagocytosis, promote the release of NO and increase the release of cytokines. At present, most of the research on chia seed polysaccharides by domestic and

foreign scholars is concentrated in the part of its emulsification, water holding capacity, viscosity and partial structure research of polysaccharides. There have been few reports of establishing a systematic method for extraction, separation and purification, structural characterization, and pharmacological activity analysis to study chia seed polysaccharides. In summary, the authors hope to enrich the material basis research of chia seed polysaccharides through the experimental results of this study, and lay a foundation for the further development and utilization of chia seeds.

Funding

This research did not receive any specific grant from funding agencies in the public, commercial, or not-for-profit sectors.

CRediT authorship contribution statement

Zhijun Xiao: Conceptualization, Methodology, Validation, Formal analysis. Changyang Yan: Conceptualization, Methodology, Validation, Formal analysis. Chunxue Jia: Writing – original draft, Writing – review & editing. Ying Li: Writing – original draft, Writing – review &

editing. **Yuanlin Li:** Writing – original draft, Writing – review & editing. **Jie Li:** Writing – original draft, Writing – review & editing. **Xinxin Yang:** Writing – original draft, Writing – review & editing. **Xueyan Zhan:** Investigation, Resources, Supervision, Project administration. **Changhua Ma:** Investigation, Resources, Supervision, Project administration.

Declaration of Competing Interest

The authors declare that they have no known competing financial interests or personal relationships that could have appeared to influence the work reported in this paper.

Data availability

Data will be made available on request.

Appendix A. Supplementary data

Supplementary data to this article can be found online at <https://doi.org/10.1016/j.fochx.2023.101011>.

References

- Abdel-Akher, M., Hamilton, J. K., Montgomery, R., & Smith, F. (1952). A new procedure for the determination of the fine structure of polysaccharides. *Journal of the American Chemical Society*, 74(19), 4970–4971.
- Alfredo, V. O., Gabriel, R. R., Luis, C. G., & David, B. A. (2009). Physicochemical properties of a fibrous fraction from chia (*Salvia hispanica L.*). *LWT - Food Science and Technology*, 42(1), 168–173.
- Ayerza, R., & Coates, W. (2004). Composition of chia (*Salvia hispanica*) grown in six tropical and subtropical ecosystems of South America. *Tropical Science*, 44(03), 131–135.
- Bai, R. B., Ma, Y. L., & Zhang, P. (2017). The content of sugar in polysaccharides containing galacturonic acid was determined by phenol-sulfuric acid method combined with correction factor method. *Chinese Pharmacy*, 28(21), 2974–2978.
- Blumenkrantz, N., & Asboe-Hansen, G. (1973). New method for quantitative determination of uronic acids. *Analytical Biochemistry*, 54(02), 484–489.
- Bornik, M. A., & Kroh, L. W. (2013). D-galacturonic acid as a highly reactive compound in nonenzymatic browning. 1. Formation of browning active degradation products. *Journal of Agricultural and Food Chemistry*, 61(14), 3494–3500.
- Bystrova, O. V., Zatonsky, G. V., Borisova, S. A., Kocharova, N. A., Shashkov, A. S., Knirel, Y. A., ... Stanislavskii, E. S. (2000). Structure of an acidic O-specific polysaccharide of the bacterium *Providencia alcalifaciens* O7. *Biochemistry*, 65(6), 677–684.
- Capitani, M. I., Corzo-Rios, L. J., Chel-Guerrero, L. A., Betancur-Ancona, D. A., Nolasco, S. M., & Tomás, M. C. (2015). Rheological properties of aqueous dispersions of chia (*Salvia hispanica L.*) mucilage. *Journal of Food Engineering*, 149, 70–77.
- Castell, J. V., Andus, T., Kunz, D., & Heinrich, P. C. (1989). Interleukin-6: The major regulator of acute-phase protein synthesis in man and rat. *Annals of the New York Academy of Sciences*, 557(1), 87–101.
- Castric, P., Cassels, F. J., & Carlier, R. W. (2001). Structural characterization of the *Pseudomonas aeruginosa* 1240 pilin glycan. *Journal of Biological Chemistry*, 276(28), 26479–26485.
- Chen, X., Li, T., Qing, D., Chen, J., Zhang, Q., & Yan, C. (2020). Structural characterization and osteogenic bioactivities of a novel *Humulus lupulus* polysaccharide. *Food & Function*, 11(01), 1165–1175.
- Cheng, A. W. (2008). Extraction of *glycyrrhiza* polysaccharides and immune regulation of mouse peritoneal macrophages. Jiangnan University.
- Fan, J., Feng, H., Yu, Y., Sun, M. X., Liu, Y. R., Li, T. Z., & Sun, M. D. (2017). Antioxidant activities of the polysaccharides of Chuanminshen violaceum. *Carbohydrate Polymers*, 157, 629–636.
- Feng, S., Luan, D., Ning, K., Shao, P., & Sun, P. (2019). Ultrafiltration isolation, hypoglycemic activity analysis and structural characterization of polysaccharides from *Brasenia schreberi*. *International Journal of Biological Macromolecules*, 135, 141–151.
- Fernandes, S. S., & Mercedes Salas-Mellado, M. D. L. (2017). Addition of chia seeds mucilage for reduction of fat content in bread and cakes. *Food Chemistry*, 227, 237–244.
- Ganter, J. J., Léa, M. S., Heyraud, A., Petkowicz, C. L. O., Rinaudo, M., & Reicher, F. (1995). Galactomannans from Brazilian seeds: Characterization of the oligosaccharides produced by mild acid hydrolysis. *International Journal of Biological Macromolecules*, 17, 13–19.
- Goh, K. K. T., Matia-Merino, L., Chiang, J. H., Quek, R., Soh, S. J. B., & Lentele, R. G. (2016). The physico-chemical properties of chia seeds polysaccharide and its microgel dispersion rheology. *Carbohydrate Polymers*, 149, 297–307.
- Gong, G. P., Dang, T. T., Deng, Y. N., Han, J. L., Zou, Z. H., Jing, S., ... Wang, Z. F. (2018). Physicochemical properties and biological activities of polysaccharides from *Lycium barbarum* prepared by fractional precipitation. *International Journal of Biological Macromolecules Structure Function & Interactions*, 109, 611–618.
- Hui, H., Li, X., Jin, H., Yang, X., Xin, A., Zhao, R., & Qin, B. (2019). Structural characterization, antioxidant and antibacterial activities of two heteropolysaccharides purified from the bulbs of *Lilium davidii* var. *unicolor* Cotton. *International Journal of Biological Macromolecules*, 133, 306–315.
- Ixtaina, V. Y., Nolasco, S. M., & Tomás, M. C. (2008). Physical properties of chia (*Salvia hispanica L.*) seeds. *Industrial Crops and Products*, 28(03), 286–293.
- Jahanbin, K., Abbasian, A., & Ahang, M. (2017). Isolation, purification and structural characterization of a new water-soluble polysaccharide from *Eremurus stenophyllus* (boiss. & buhse) baker roots. *Carbohydrate Polymers*, 178, 386–393.
- Jia, X., Zhang, C., Qiu, J., Wang, L., Bao, J., Wang, K., ... He, C. (2015). Purification, structural characterization and anticancer activity of the novel polysaccharides from *Rhynchosia minima* root. *Carbohydrate Polymers*, 132, 67–71.
- Kohno, J., Asai, Y., Nishio, M., Sakurai, M., Kawano, K., Hiramatsu, H., ... Komatsubara, S. (1999). TMC-171A, B, C and TMC-154, novel polyketide antibiotics produced by *Gliocladium* sp. TC 1304 and TC 1282. *The Journal of Antibiotics*, 52(19), 1114–1123.
- Kou, F., Ge, Y. F., Wang, W. H., Mei, Y. X., Cao, L. K., Wei, X. T., ... Wu, X. (2023). A review of *Ganoderma lucidum* polysaccharides: Health benefit, structure-activity relationship, modification, and nanoparticle encapsulation. *International Journal of Biological Macromolecules*, 243, Article 125199.
- Kuang, M. T., Li, J. Y., Yang, X. B., Yang, L., Xu, J. Y., Yan, S., ... Zhou, J. (2020). Structural characterization and hypoglycemic effect via stimulating glucagon-like peptide-1 secretion of two polysaccharides from *Dendrobium officinale*. *Carbohydrate Polymers*, 241, Article 116326.
- Lin, K. Y., Daniel, J. R., & Whistler, R. L. (1994). Structure of chia seeds polysaccharide exudate. *Carbohydrate Polymers*, 23(1), 13–18.
- Lu, Y., Xu, L., Cong, Y., Song, G., Han, J., Wang, G., ... Chen, K. (2019). Structural characteristics and anticancer/antioxidant activities of a novel polysaccharide from *Trichoderma kanganensis*. *Carbohydrate Polymers*, 205, 63–71.
- Luo, L., Zheng, S., Huang, Y., Qin, T., Xing, J., Niu, Y. L., ... Wang, D. Y. (2016). Preparation and characterization of Chinese yam polysaccharide PLGA nanoparticles and their immunological activity. *International Journal of Pharmaceutics*, 511(01), 140–150.
- Marinelli, R., Moura, C. S., Moraes, É., Lenquiste, S. A., Lollo, P., Morato, P. N., ... Maróstica, M. R. (2015). Chia (*Salvia hispanica L.*) enhances HSP, PGC-1α expressions and improves glucose tolerance in diet-induced obese rats. *Nutrition*, 31(5), 740–748.
- McNally, D. J., Lamoureux, M. P., Karlyshev, A. V., Fiori, L. M., Brisson, J. R., Jarrell, H. C., ... Szymanski, C. M. (2007). Commonality and biosynthesis of the O-methyl phosphoramidate capsule modification in *Campylobacter jejuni*. *Journal of Biological Chemistry*, 282(39), 28566–28576.
- Naugler, W. E., & Karin, M. (2008). The wolf in sheep's clothing: The role of interleukin-6 in immunity, inflammation and cancer. *Trends in Molecular Medicine*, 14(3), 109–119.
- Nep, E. I., & Conway, B. R. (2010). Characterization of grewia gum, a potential pharmaceutical excipient. *Journal of Excipients and Food Chemicals*, 1(1), 30–40.
- Ogawa, K., Wanatabe, T., Tsurugi, J., & Ono, S. (1972). Conformational behavior of a gel-forming (1→3)-β-D-glucan in alkaline solution. *Carbohydrate Research*, 23(03), 399–405.
- Rafaela, D. S. M., Lenquiste, S. A., Moraes, E. A., & Maróstica, M. (2015). Antioxidant potential of dietary chia seeds and oil (*Salvia hispanica L.*) in diet-induced obese rats. *Food Research International*, 76, 666–674.
- Ren, Z. Y., Liu, A. P., Chen, X. H., Wang, X., Liu, Q., ... Shen, R. (2018). The modified M-hydroxybiphenyl method was used to determine the content of uronic acid in pneumococcal capsular polysaccharide. *Chinese Journal of New Medicine*, 27(06), 644–649.
- Rossi, A. S., Oliva, M. E., Ferreira, M. R., Chicco, A., & Lombardo, Y. B. (2013). Dietary chia seed induced changes in hepatic transcription factors and their target lipogenic and oxidative enzyme activities in dyslipidaemic insulin-resistant rats. *British Journal of Nutrition*, 109(09), 1617–1627.
- Saitô, H., Yoshioka, Y., Uehara, N., Aketagawa, J., Tanaka, S., & Shibata, Y. (1991). Relationship between conformation and biological response for (1→3)-β-d-glucans in the activation of coagulation Factor G from limulus amebocyte lysate and host-mediated antitumor activity. Demonstration of single-helix conformation as a stimulant. *Carbohydrate Research*, 217, 181–190.
- Shimoyama, A., Di Lorenzo, F., Yamaura, H., Mizote, K., Palmigiano, A., Pither, M., ... Fukase, K. (2021). Lipopolysaccharide from gut-associated lymphoid-tissue-resident Alcaligenes faecalis: Complete structure determination and chemical synthesis of its lipid A. *Angewandte Chemie*, 60(18), 10023–10031.
- Steffolani, E., Martinez, M. M., León, A., & Gómez, M. (2015). Effect of pre-hydration of chia (*Salvia hispanica L.*) seeds and flour on the quality of wheat flour breads. *LWT-Food Science and Technology*, 61(2), 401–406.
- Tabarsa, M., You, S. G., Abedi, M., Ahmadian, N., Li, C. S., & Talapphet, N. (2019). The activation of RAW264.7 murine macrophage and natural killer cells by glucomannogalactan polysaccharides from *Tornabea scutellifera*. *Carbohydrate Polymers*, 219, 368–377.
- Tan, C., Wang, Y. X., & Chen, D. (2023). Natural polysaccharides protect against diet-induced obesity by improving lipid metabolism and regulating the immune system. *Food Research International*, 172, Article 113192.
- Timilsena, Y. K. P., Adhikari, R., Kasapis, S., & Adhikari, B. (2016). Molecular and functional characteristics of purified gum from Australian Chia seeds. *Carbohydrate Polymers: Scientific and Technological Aspects of Industrially Important Polysaccharides*, 136, 128–136.

- Toscano, L. T., Silva, C. S. O., Toscano, L. T., Almeida, A. E. M., Santos, A. C., & Silva, A. S. (2014). Chia flour supplementation reduces blood pressure in hypertensive subjects. *Plant Foods for Human Nutrition*, 69(04), 392–398.
- Uribe, J., Perez, J., Kaul, H. C., Rubio, G. R., & Alcocer, C. G. (2011). Extraction of oil from Chia seeds with supercritical CO₂. *The Journal of Supercritical Fluids*, 56(2), 174–178.
- Vinogradov, E., Frirdich, E., MacLean, L. L., Perry, M. B., Petersen, B. O., Duus, J. O., ... Whitfield, C. (2002). Structures of lipopolysaccharides from Klebsiella pneumoniae. Elucidation of the structure of the linkage region between core and polysaccharide O chain and identification of the residues at the non-reducing termini of the O chains. *Journal of Biological Chemistry*, 277(28), 25070–25081.
- Vladimir, V., Dana, W., John, L. S., Alexandra, L. J., Alexander, L. R., Richard, P. B., ... Amir, H. (2007). Supplementation of conventional therapy with the novel grain Salba (*Salvia hispanica* L.) improves major and emerging cardiovascular risk factors in type 2 diabetes: Results of a randomized controlled. *Diabetes Care*, 30(11), 2804–2810.
- Wang, D. D., Wang, W. B., Wang, P., Wang, C., Niu, J. T., Liu, Y., & Chen, Y. Z. (2023). Research progress of colon-targeted oral hydrogel system based on natural polysaccharides. *International Journal of Pharmaceutics*, 643, Article 123222.
- Wei, W., Xiao, H. T., Bao, W. R., Ma, D. L., Leung, C. H., Han, X. Q., ... Han, Q. B. (2016). TLR-4 may mediate signaling pathways of Astragalus polysaccharides RAP induced cytokine expression of RAW264.7 cells. *Journal of Ethnopharmacology*, 179, 243–252.
- Wu, Q., Luo, M., Yao, X., & Yu, L. (2020). Purification, structural characterization, and antioxidant activity of the COP-W1 polysaccharide from Codonopsis tangshen Oliv. *Carbohydrate Polymers*, 236, Article 116020.
- Xie, J. H., Xin, L., Shen, M. Y., Nie, S. P., Hui, Z., Li, C., ... Xie, M. Y. (2013). Purification, physicochemical characterisation and anticancer activity of a polysaccharide from Cyclocarya paliurus leaves. *Food Chemistry*, 136(3–4), 1453–1460.
- Xu, J. (2019). *Study on purification, properties and biological activity of extracellular polysaccharide from Fusarium fusarium*. Northeast Normal University.
- Xu, Y., Niu, X., Liu, N., Gao, Y., Wang, L., Xu, G., ... Yang, Y. (2018). Characterization, antioxidant and hypoglycemic activities of degraded polysaccharides from blackcurrant (*Ribes nigrum* L.) fruits. *Food Chemistry*, 243, 26–35.
- Yuge, N., Pingping, S., Lei, C., Hua, Z., Lu, G., Xiaowei, Z., ... Yu, L. L. (2014). Characterization of a novel alkali-soluble heteropolysaccharide from tetraploid *Gynostemma pentaphyllum* Makino and its potential anti-inflammatory and antioxidant properties. *Journal of Agricultural And Food Chemistry*, 62(17), 3783–3790.
- Zhang, S. A., Liu, H. Y., & Li, W. (2023). Polysaccharide-based hydrogel promotes skin wound repair and research progress on its repair mechanism. *International Journal of Biological Macromolecules*, 248, Article 125949.
- Zhang, S., Zhang, Q., An, L., Zhang, J., & Guo, Y. (2019). A fructan from *Anemarrhena asphodeloides* Bunge showing neuroprotective and immunoregulatory effects. *Carbohydrate Polymers*, 229(8), Article 115477.
- Zhou, C., Mi, S., Li, J., Gao, J., & Sang, Y. (2020). Purification, characterisation and antioxidant activities of chondroitin sulphate extracted from *Raja porosa* cartilage. *Carbohydrate Polymers*, 241, Article 116306.
- Zhu, Y., Li, Q., Mao, G., Zou, Y. E., Feng, W., Zheng, D., ... Wu, X. (2014). Optimization of enzyme-assisted extraction and characterization of polysaccharides from *Hericium erinaceus*. *Carbohydrate Polymers*, 101, 606–613.